JOURNAL OF APPLIED ELECTROCHEMISTRY 21 (1991) 537–542

Mass transfer at the gas evolving inner electrode of a concentric cylindrical reactor

M. F. EL-SHERBINY, A. A. ZATOUT, M. HUSSIEN, G. H. SEDAHMED*

Chemical Engineering Department, Faculty of Engineering, Alexandria University, Alexandria, Egypt

Received 1 October 1990; revised 10 December 1990

Mass transfer coefficients for an oxygen evolving vertical PbO_2 coated cylinder electrode were measured for the anodic oxidation of acidified ferrous sulphate above the limiting current. Variables studied included the ferrous sulphate concentration, the anode height, the oxygen discharge rate and the anode surface roughness. The mass transfer coefficient was found to increase with increasing O_2 discharge rate, V, and electrode height, h, according to the proportionality expression $K \propto V^{0.34}h^{0.2}$. Surface roughness with a peak to valley height up to 2.6 mm was found to increase the rate of mass transfer by a modest amount which ranged from 33.3 to 50.8% depending on the degree of roughness and oxygen discharge rate. The present data, as well as previous data at vertical oxygen evolving electrodes where bubble coalescence is negligible, were correlated by the equation $J = 7.63\ (Re.Fr)^{-0.12}$, where J is the mass transfer J factor $(St.Sc^{0.66})$.

Notation

a_1, a_2	constants
A	electrode area (cm^2)
C	concentration of Fe^{2+} (M)
d	bubble diameter (cm)
D	diffusivity ($cm^2\ s^{-1}$)
e	electrochemical equivalent ($g\ C^{-1}$)
F	Faraday's constant
g	acceleration due to gravity ($cm\ s^{-2}$)
h	electrode height (cm)
$I_{Fe^{2+}}$	current consumed in Fe^{2+} oxidation A
I_{O_2}	current consumed in O_2 evolution, A
K	mass transfer coefficient ($cm\ s^{-1}$)
m	amount of Fe^{2+} oxidized (g)
P	gas pressure (atm)
p	pitch of the threaded surface (cm)
Q	volume of oxygen gas passing any point at the electrode surface ($cm^3\ s^{-1}$)
R	gas constant ($atm\ cm^3\ mol^{-1}\ K^{-1}$)
r	peak-to-valley height of the threaded surface (cm)
t	time of electrolysis (s)
T	temperature (K)
μ	solution viscosity ($g\ cm^{-1}\ s^{-1}$)
V	oxygen discharge velocity as defined by Equation 3 ($cm\ s^{-1}$)
Z	number of electrons involved in the reaction
Sh	Sherwood number (Kd/D)
Re	Reynolds number $(\rho Vd/\mu)$
Sc	Schmidt number (ν/D)
J	mass transfer J factor $(St.Sc^{0.66})$
St	Stanton number (K/V)
Fr	Froude number (V^2/dg)
ρ	Solution density, $g\ cm^{-3}$
ν	Kinematic viscosity ($cm^2\ s^{-1}$)
ϕ	bubble geometrical parameter defined in [31]
θ	fractional surface coverage
δ	diffusion layer thickness (cm)

1. Introduction

Although much work has been done on the effect of gas evolution on the rate of mass transfer, current distribution and ohmic drop in the parallel plate reactor [1, 2], little has been done on other geometries of practical importance such as the annular geometry which has the advantage of uniform primary current and potential distribution. The object of the present work is to study the effect of oxygen evolution on the rate of mass transfer at a vertical cylinder anode surrounded by a vertical tubular anode in relation to anode height, oxygen discharge rate and surface roughness of the anode. This would assist in predicting the rate of mass transfer, not only at stationary vertical cylinders, but also at gas evolving rotating cylinders and gas evolving annular flow reactors used in conducting diffusion controlled reactions accompanied by gas evolution, as in the case of electrosynthesis and electrochemical waste water management. Vogt [3] has shown that for gas evolving rotating cylinders the overall mass transfer coefficient may be predicted in terms of the mass transfer coefficient due to gas evolution and the mass transfer coefficient due to rotation, the same rule applies to gas evolving flow reactors [4–6].

* Author to whom all correspondence should be addressed.

0021-891X/91 $03.00 + .12

The present study was conducted using the anodic oxidation of acidified $FeSO_4$ at a PbO_2 coated lead anode which is a diffusion controlled reaction [7]. The reaction is of a special environmental importance for the removal of $FeSO_4$ from industrial waste solutions by anodic oxidation of $FeSO_4$ to $Fe_3(SO_4)_2$ prior to iron precipitation as $Fe(OH)_3$ with lime. Examples of industrial waste solutions which contain acidic $FeSO_4$ are coal mining waste solutions and steel acid pickling waste solutions. The fact that these solutions are extremely dilute and highly acidic leads to simultaneous oxygen evolution during anodic oxidation of these solutions [8, 9]. The present study is also of relevance to electrowinning of metals from solutions containing Fe^{2+} impurity where it was found that the rate of Fe^{2+} oxidation at the oxygen evolving PbO_2 anode affects the cathode current efficiency [10, 11]. Therefore, apart from the general nature of the present study, it is of special value for the problem of electrolytic iron removal from industrial effluents, and electrowinning of metals from solutions containing Fe^{2+} as impurity.

2. Experimental technique

The apparatus consisted of a cell and electrical circuit. The cell consisted of a Plexyglass container of 11.6 cm diameter and 17 cm height divided into two compartments by a porous cylindrical PVC diaphragm of 7.8 cm diameter. The porous diaphragm was fixed to the bottom of the cell by a layer of wax. The anode, which was positioned in the centre of the cell, consisted of a 1.9 cm diameter PbO_2 coated lead cylinder. The active anode height ranged from 2 to 8 cm, and was adjusted by isolating the undesired part with a Teflon tape. The bottom of each anode was isolated with epoxy resin. One smooth and four rough anodes were used. Roughness was created by cutting 60° V-threads in the lead cylinder. Table 1 gives the roughness parameters for the four surfaces. A cylindrical stainless steel screen was placed in the outer compartment as a cathode. The electrical circuit consisted of a 10 V d.c. power supply with a voltage regulator connected in series with a multirange ammeter and the cell. A high impedance voltmeter was connected in parallel with the cell to measure its voltage.

Before each run 450 and 550 cm^3 of the solution were placed in the anode and cathode compartment, respectively; care was taken that the solution level was the same in the two compartments. The solution consisted of 1.5 M H_2SO_4 and xM $FeSO_4$, where x = 0.1 or 0.2 or 0.3 M. All solutions were prepared from AR grade chemicals. Electrolysis was conducted at a constant current for a time which ranged from 5 to 8 min; current densities at which electrolysis was conducted ranged from 0.025 to 0.0628 A cm^2. At the end of electrolysis a sample of 10 cm^3 was taken from the inner compartment for analysis by titration against 0.01 M $KMnO_4$ solution [12]. The amount of $FeSO_4$ oxidized during electrolysis ranged from 3 to 5%. The current consumed in $FeSO_4$ oxidation, $I_{Fe^{2+}}$, was

Table 1. Effect of surface roughness on cell voltage and current efficiency at different current densities. $[FeSO_4]$ = 0.2 *M; electrode height* = 8 *cm*

Anode roughness	c.d. × 10^3 (A cm^{-2})	Cell voltage (V)	Current efficiency
Smooth	25.12	2.42	0.633
	31.40	2.46	0.579
	37.68	2.52	0.523
	43.96	2.60	0.483
	50.24	2.65	0.452
	56.52	2.70	0.415
	62.80	2.74	0.386
R_1, r = 0.6 mm, p = 1.25 mm	25.12	2.46	0.687
	31.40	2.43	0.603
	37.68	2.58	0.563
	43.96	2.63	0.526
	50.24	2.68	0.490
	56.52	2.70	0.456
	62.80	2.75	0.425
R_2, r = 1.25 mm, p = 1.75 mm	25.12	2.45	0.762
	31.40	2.49	0.718
	37.68	2.56	0.673
	43.96	2.61	0.646
	50.24	2.68	0.596
	56.52	2.71	0.556
	62.80	2.75	0.516
R_3, r = 2 mm, p = 2.5 mm	25.12	2.41	0.814
	31.40	2.48	0.754
	37.68	2.58	0.704
	43.96	2.62	0.663
	50.24	2.67	0.618
	56.52	2.72	0.596
	62.80	2.76	0.561
R_4, r = 2.6 mm, p = 3.5 mm	25.12	2.42	0.859
	31.40	2.49	0.796
	37.68	2.58	0.744
	43.96	2.63	0.685
	50.24	2.69	0.648
	56.52	2.75	0.617
	62.80	2.79	0.585

calculated from the analytically determined amount of oxidized Fe^{2+} using Faraday's law

$$m = eI_{Fe^{2+}}t \quad (1)$$

The mass transfer coefficient, K, of $FeSO_4$ oxidation was calculated from the equation

$$K = \frac{I_{Fe^{2+}}}{AZFC} \quad (2)$$

In the case of rough electrodes the projected area, A, rather than the true area was used in calculating the mass transfer coefficient. The oxygen discharge rate, V, was calculated from the current consumed in oxygen discharge, I_{O_2}, using Faraday's law and the gas law

$$V = I_{O_2}RT/4FPA \quad (3)$$

The quantity I_{O_2}, was obtained by subtracting the current consumed in Fe^{2+} oxidation from the total cell current. Each run was conducted twice using a fresh solution. The temperature was 25 ± 1°C. The vis-

cosity and density of the solution required to correlate the data were determined by an Ostwald viscometer and a density bottle, respectively [13].

Although chemical oxidation of acidic $FeSO_4$ by oxygen or air is known to be extremely slow [14], an experiment was conducted to confirm this fact under the present conditions by bubbling oxygen through the solution for 10 min, no oxidation was found to take place. Accordingly $FeSO_4$ oxidation during electrolysis takes place only by anodic oxidation without interference from chemical oxidation. PbO_2 coated lead anodes were prepared by anodic oxidation of lead cylinders as mentioned elsewhere [7, 15].

3. Results and discussions

Figure 1 shows the effect of oxygen discharge rate on the mass transfer coefficient of the anodic oxidation of Fe^{2+} at different ferrous sulphate concentrations, the data fit the equation

$$K = a_1 V^{0.34} \tag{4}$$

The exponent 0.34 agrees well with the prediction of the hydrodynamic model [16] and the surface renewal model [17]. It would be of interest from a mechanistic point of view to compare the present data and the data of Sedahmed [18]. The latter was obtained by measuring the mass transfer coefficient for the cathodic deposition of copper from acidified copper sulphate solution at a vertical cylinder cathode stirred by oxygen evolving at a vertical cylinder lead anode placed below the cylinder cathode and flush with it. Figure 1 shows that the mass transfer coefficient at the gas evolving electrode is higher than that at the none gas-evolving cathode by an amount ranging from 78 to 82%. This difference may be attributed to: (i) microconvection induced by bubble growth and detachment which operates along with macroconvection at the gas evolving electrode, whilst (ii) the magnitude of macroconvection increases along the gas evolving electrode due to bubbles coming from below.

Figure 2 shows that the mass transfer coefficient increases with anode height according to the equation

$$K = a_2 h^{0.2} \tag{5}$$

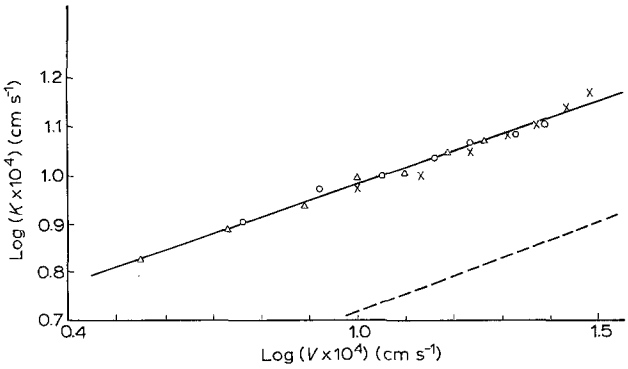

Fig. 1. Effect of oxygen discharge rate on the mass transfer coefficient at different ferrous sulphate concentrations. Electrode height = 8 cm. (– – – –) Oxygen sparged electrode [18]; (———) oxygen evolving electrode. [$FeSO_4$]: (×) 0.1, (○) 0.2 and (△) 0.3 M.

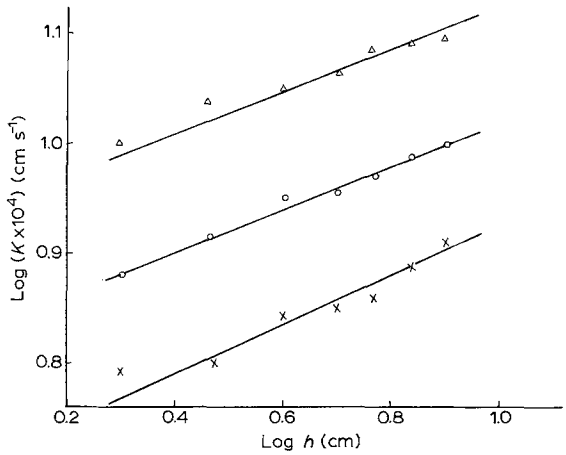

Fig. 2. Effect of anode height on the mass transfer coefficient at different oxygen discharge rates. [$FeSO_4$] = 0.2 M. $V \times 10^4$ cm s^{-1}. (×) 7.15, (○) 12.8, and (△) 22.24.

This result could be explained on the basis that height has two opposing effects on the mass transfer coefficient. According to the hydrodynamic model the mass transfer tends to decrease with increasing electrode height, for short oxygen evolving anodes in acid solution (1 mm < h < 16 mm). Janssen and Hoogland [10] found that the mass transfer coefficient decreases with anode height according to the expression

$$K \propto h^{-0.13} \tag{6}$$

Assuming uniform current distribution along the electrode, the volume of oxygen gas, Q, passing any point on the electrode surface per second increases with increasing electrode height with a consequent increase in the mass transfer coefficient, this effect may be expressed mathematically as follows:
According to the hydrodynamic model

$$K \propto Q^{0.33} \tag{7}$$

but since $Q \propto h$, then

$$K \propto h^{0.33} \tag{8}$$

combining equations (6) and (8) it follows that

$$K \propto h^{0.2} \tag{9}$$

which agrees closely with the present data as represented by Equation 5.

As an alternative to Equation 6, the dependence of the mass transfer coefficient on electrode height due to the build up of a hydrodynamic boundary layer can be obtained from the mass transfer equation representing turbulent developing single phase liquid flow, namely [19]

$$K \propto h^{-0.2} \tag{10}$$

Combining equations (8) and (10) it follows that

$$K \propto h^{0.13} \tag{11}$$

which is in a fair agreement with Equation 5. It should be emphasized that the above argument is valid only for conditions under which mass is transferred mainly by macroconvection. For conditions where bubble coalescence at the electrode surface is significant, as

in the case of oxygen discharge from alkaline solution [20] or where microconvection is predominating (e.g. at high current densities), it is expected that the effect of electrode height on the mass transfer coefficient would be different from that reported here. Venczel [21], who studied mass transfer at hydrogen evolving electrodes ranging in height from 1 to 20 cm using acid solution, found that electrode height has no effect on the rate of mass transfer. Recently Janssen [22] found that the mass transfer coefficient of the cathodic reduction of $K_3Fe(CN)_6$ in alkaline solution at a hydrogen evolving electrode decreases with height and then remains constant with further increase in height. For an oxygen evolving electrode he found that the mass transfer coefficient for the anodic oxidation of $K_4Fe(CN)_6$ in alkaline solution is independent of height. In this case the electrode height ranged from 0.5 to 16 cm.

Figure 3 shows the effect of anode roughness on the mass transfer coefficient which was found to increase over the value at the smooth anode by an amount ranging from 33.3 to 50.8% depending on the peak-to-valley height of the thread and oxygen discharge rate. To explain the effect of surface roughness on the mass transfer coefficient, the equivalent diffusion layer thickness, δ, was calculated from $K = D/\delta$ with $D_{Fe^{2+}} = 5.13 \times 10^{-6}$ [23]. Under the present conditions δ ranged from 0.027 to 0.057 mm. A comparison between the values of δ and the values of the peak-to-valley height (r) shown in Table 1 indicates that all roughness elements used in the present work protrude outside the diffusion layer thereby increasing the effective anode area. A comparison between the percentage increase in the mass transfer coefficient (33.3–50.8%) and the percentage increase in the true electrode area of the rough anodes (35.8–79%) reveals that under the present conditions mass transfer enhancement through turbulence promotion by the roughness elements is negligible. Sedahmed and Shemilt [24], who studied forced convection mass transfer at the threaded inner core of an annulus found that the rate of mass transfer increases in the turbulent flow regime by a factor ranging from 1.125 to 4.3 depending on peak-to-valley height and solution flow rate. The authors used electrodes with peak-to-valley height ranging from 0.025 to 1.648 mm and a Reynolds number range of 3 700–30 000. The inability of roughness elements to enhance the rate of mass transfer through turbulence promotion at gas evolving electrodes may be due to the fact that the intensity of turbulence generated by oxygen bubbles is already high at the gas evolving electrode. Fouad *et al.* [25] studied the combined effect of surface roughness and oxygen evolution on the mass transfer coefficient of the anodic oxidation of alkaline $K_4Fe(CN)_6$ at a vertical nickel plate in which horizontal grooves were machined, all roughness elements protruded outside the diffusion layer. They found that surface roughness results in a decrease in the rate of mass transfer at oxygen evolving electrodes except at low degrees of roughness and high discharge rate. They explained the decrease in the rate of mass transfer by the fact that a considerable part of the active area of the electrode becomes blanketed with oxygen bubbles residing inside the grooves. The release of these bubbles by buoyancy is hindered by their location inside the grooves. A comparison between the results of Fouad *et al.* and the present results shows that the geometry of the roughness elements plays an important role and roughness should be designed in practice in such a way as to facilitate bubble release.

Previous studies [26, 27] on the effect of microroughness with roughness elements submerged in the diffusion layer have shown that microroughness has no effect on the rate of mass transfer at gas evolving electrodes.

To further evaluate the effect of surface roughness on the performance of the gas evolving cell, power consumption was calculated for different degrees of

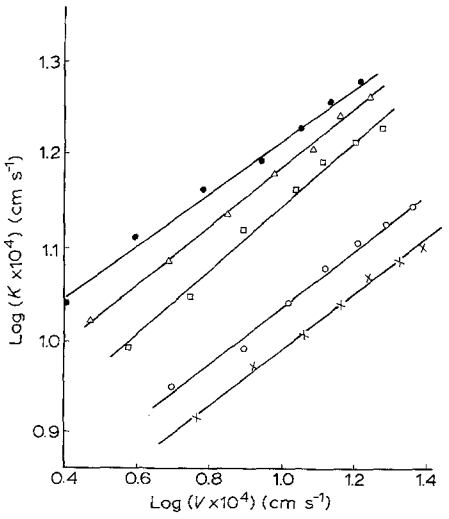

Fig. 3. Effect of oxygen discharge rate on the mass transfer coefficient at different degrees of anode surface roughness. [$FeSO_4$] = 0.2 M. Anode height = 8 cm. Degree of roughness: (×) smooth, (○) R_1, (□) R_2, (△) R_3, and (●) R_4.

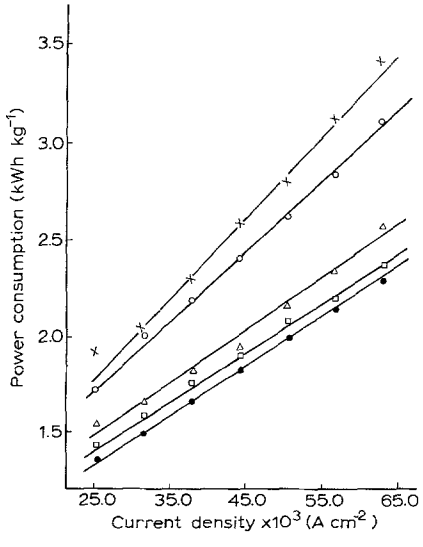

Fig. 4. Effect of current density on power consumption at different degrees of anode surface roughness [$FeSO_4$] = 0.2 M. Anode height = 8 cm. Degree of roughness: (×) smooth, (○) R_1, (□) R_2, (△) R_3, and (●) R_4.

roughness at different current densities. Figure 4 shows that power consumption in kWh kg^{-1} decreases with increasing surface roughness. This decrease in power consumption is the outcome of two opposing effects for surface roughness, Table 1 shows that surface roughness increases the total cell voltage, probably because macroroughness hinders the early release of oxygen bubbles with a consequent increase in the ohmic drop. On the other hand Table 1 shows that the current efficiency increases with increasing surface roughness as a result of increase of the mass transfer coefficient (Fig. 4). The decrease in power consumption with increasing surface roughness shows that the beneficial effect on current efficiency outweighs the adverse effect on cell voltage. The increase in cell voltage at rough electrodes is consistent with the results of Kuhn *et al.* [28, 29], who found that electrode roughening increases the H_2 overpotential. The authors attributed this phenomenon to the decrease in electrode area as a result of the trapping of hydrogen bubbles within the surface irregularities.

4. Data correlation

In view of the complex nature of mass transfer at gas evolving electrodes little has been done to obtain an overall mass transfer correlation which can be used in the design and operation of gas evolving electrochemical reactors. Based on the penetration model of Ibl and Venczel [30], Vogt [2] developed the following correlation

$$Sh = \frac{2.76}{\phi^{0.33}} (Re \,.\, Sc)^{0.5}(1 - \theta)^{0.5} \qquad (12)$$

The microconvection model of Stephan and Vogt [31] led to the correlation

$$Sh = 0.93\, Re^{0.5} Sc^{0.49} \qquad (13)$$

The break of bubble diameter, d, was used as a characteristic length in calculating Sh and Re in Equations 12 and 13.

In a tentative attempt to obviate the need for parameters such as d, ϕ and θ used in Equations 12 and 13, the present data for smooth electrodes along with previous data [16, 32, 33] at oxygen evolving vertical electrodes were empirically correlated using the dimensionless groups, Re and Fr usually used in correlating heat and mass transfer in gas sparged systems. The physical properties of the solutions used to correlate the data were obtained from the literature [16, 31, 33]. For the conditions $800 < Sc < 2940$, $4.34 \times 10^{-15} < Fr \,.\, Re < 10.2 \times 10^{-5}$, Fig. 5 shows that the data fit the equation

$$J = 7.63\, (V^3/vg)^{-0.12} \qquad (14)$$

that is

$$J = 7.63\, (Re \,.\, Fr)^{-0.12} \qquad (15)$$

With an average deviation of $\pm 15.8\%$ which is reasonable in view of the fact that the height effect was ignored in obtaining Equation (15). It should be emphasized that: (i) Equation 15 is valid only for conditions where bubble coalescence is negligible, (ii) although Equation 15 predicts an exponent 0.36 for the dependence of the mass transfer coefficient on gas velocity which is different from the values cited by different authors, Equation 15 could serve as an approximate general design equation for oxygen evolving vertical electrodes. Equation 15 should be used only within the aforementioned range of conditions as extrapolation may lead to a considerable error.

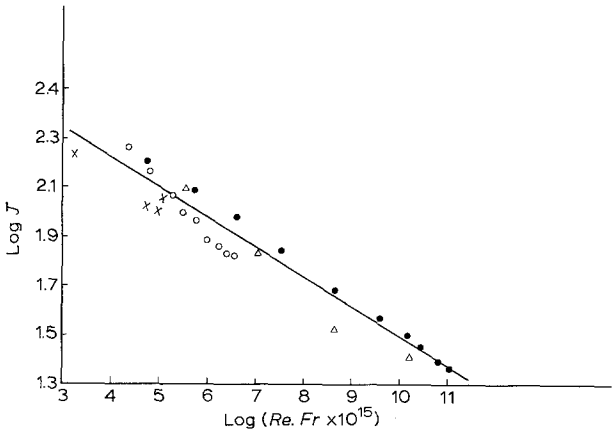

Fig. 5. Overall mass transfer correlation at vertical oxygen evolving electrodes system and reference. (×) chlorate formation [32], (○) Fe^{2+} oxidation (present work), (△) Ce^{3+} oxidation [16], and (●) Ce^{3+} oxidation [33].

References

[1] P. Sides, in 'Modern Aspects of Electrochemistry', (Vol. 18, edited by R. E. White, J. O'M. Bockris and B. E. Conway), Plenum Press, New York (1986) pp. 303.
[2] H. Vogt, in 'Comprehensive Treatise of Electrochemistry', (Vol. 6, edited by E. Yeager, J. O'M. Bockrise, B. E. Conway and S. Sarangapani), Plenum Press, New York (1983) p. 445.
[3] H. Vogt, *Electrochim Acta* **23** (1978) 203.
[4] *Idem, ibid.* **32** (1987) 633.
[5] M. D. Birkett and A. Kuhn, *ibid.* **22** (1977) 1427.
[6] G. Bendrich, W. Seiler and H. Vogt, *Int. J. Heat Mass Transfer* **29** (1986) 1741.
[7] J. A. Harrison and J. M. Mayne, *Electrochim Acta* **28** (1983) 1223.
[8] G. B. Adams, R. P. Hollandsworth and D. N. Bennion, *J. Electrochem. Soc.* **122** (1975) 1043.
[9] *Idem, AIChE Symposium Series* **73** (1976) 99.
[10] D. W. Dew and C. V. Philips, *Hydrometallurgy* **14** (1985) 331.
[11] *Idem, ibid.* **14** (1985) 351.
[12] A. I. Vogel, 'A Text Book of Quantitative Inorganic Analysis', 3rd Edition, Longmans, London (1961).
[13] A. Findlay and J. A. Kitchener, 'Practical physical Chemistry', 8th Edition, Longmans, London (1965).
[14] Harvard University, 'Report, Water Pollution Control Research Series', 14010 FMH 12/70, Dec. 1960, EPA, Washington, DC.
[15] J. S. Clarke, R. E. Ehigamusoe and A. T. Kuhn, *J. Electroanal. Chem.* **70** (1976) 333.
[16] L. J. J. Janssen and J. G. Hoogland, *Electrochim Acta* **15** (1970) 1013.
[17] G. H. Sedahmed, *J. Appl. Electrochem.* **17** (1987) 746.
[18] *Idem, ibid.* **14** (1984) 693.
[19] D. Pickett, 'Electrochemical Reactor Design', Elsevier, New York (1977) p. 139.
[20] L. J. J. Janssen and J. G. Hoogland, *Electrochim Acta* **18** (1973) 543.
[21] J. Venczel, Dissertation, ETH, Zurich (1961).

[22] L. J. J. Janssen, *J. Appl. Electrochem.* **17** (1987) 1177.
[23] G. M. Whitney and C. W. Tobias, *J. Electroanal. Chem.* **229** (1986) 429.
[24] G. H. Sedahmed and L. W. Shemilt, *Letters in Heat and Mass Transfer* **3** (1976) 499.
[25] M. G. Fouad, G. H. Sedahmed and H. El-Abd, *Electrochim. Acta* **18** (1973) 279.
[26] N. Ibl, R. Kind and E. Adam, *an. Quim.* **71** (1975) 1008.
[27] L. J. J. Janssen, *Electrochim Acta* **23** (1978) 81.
[28] A. T. Kuhn, J. Bin Yusof and P. Hogan, *J. Appl. Electrochem.* **9** (1979) 765.
[29] H. Hamza and A. T. Kuhn, *ibid.* **10** (1980) 635.
[30] N. Ibl and J. Venczel, *Metalloberflache* **24** (1970) 365.
[31] K. Stephan and H. Vogt, *Electrochim Acta* **24** (1979) 11
[32] T. R. Beck, *J. Electrochem. Soc.* **116** (1969) 1038.
[33] N. Ibl, E. Adam, J. Venczel and E. Schalch, *Chem. Ing. Tech.* **43** (1971) 202.